

Hierarchical Representation Learning in Graph Neural Networks with Node Decimation Pooling

Filippo Maria Bianchi*, Daniele Grattarola, Lorenzo Livi, Cesare Alippi

Abstract—In graph neural networks (GNNs), pooling operators compute local summaries of input graphs to capture their global properties; in turn, they are fundamental operators for building deep GNNs that learn effective, hierarchical representations. In this work, we propose the Node Decimation Pooling (NDP), a pooling operator for GNNs that generates coarsened versions of a graph by leveraging on its topology only. During training, the GNN learns new representations for the vertices and fits them to a pyramid of coarsened graphs, which is computed in a pre-processing step. As theoretical contributions, we first demonstrate the equivalence between the MAXCUT partition and the node decimation procedure on which NDP is based. Then, we propose a procedure to sparsify the coarsened graphs for reducing the computational complexity in the GNN; we also demonstrate that it is possible to drop many edges without significantly altering the graph spectra of coarsened graphs. Experimental results show that NDP grants a significantly lower computational cost once compared to state-of-the-art graph pooling operators, while reaching, at the same time, competitive accuracy performance on a variety of graph classification tasks.

Index Terms—Graph neural networks; Hierarchical pooling; Maxcut optimization; Kron reduction; Graph classification.

I. INTRODUCTION

Graph Neural Networks (GNNs) constitute a class of machine learning models that learn representations of graph-structured data to solve a large variety of inference tasks [1]. Differently from those neural networks that process input signals such as vectors, grids, or sequences, GNNs operate on arbitrary structures defined by graphs. As a consequence, standard pooling operations that leverage on the regular structure of the data and physical locality principles cannot be immediately applied to GNNs.

Graph pooling requires to aggregate the graph node features while reducing, at the same time, the underlying structure in order to maintain significant connectivity between pooled nodes. This allows performing further message-passing (MP) operations [2] after pooling, gradually distilling global properties of the graph in deeper layers of a GNN.

In this paper, we propose *Node Decimation Pooling* (NDP), a pooling operator for GNNs. NDP is based on node decimation, a procedure developed in the field of graph signal processing

for the design of multi-scale graph filters [3]. In particular, we build upon the *multi-resolution* framework [4], which consists in first subsampling the nodes of a graph and then building a coarsened graph from the remaining nodes. The NDP procedure that we propose pre-computes a *pyramid* of graph Laplacians representing the coarsened graphs at different levels of pooling, which are then used as support for the node representations learned at different depths of the GNN architecture.

The novel contributions of the work can be summarized as:

- 1) we introduce the new NDP operator and demonstrate that it allows building GNN models characterized by a low computational complexity (both in terms of time and memory) and high accuracy on several graph classification tasks;
- 2) we demonstrate that there exists a strong relationship between the MAXCUT objective and a simple spectral partitioning technique. Such a dependency is exploited in NDP to select the nodes to be discarded in order to reduce the graph size.
- 3) we propose a graph sparsification procedure that reduces the computational cost of the MP operations applied after pooling, with a minimum impact on the quality of the representations learned by the GNN model. In particular, we show that it is possible to remove a considerable amount (volume) of edges without altering too much the spectrum of the graph. To support our claim, we provide a theoretical bound that quantifies the amount of changes in the graph structure when the sparsification is applied.

When compared to other methods for graph pooling, NDP performs significantly better than similar pooling techniques that pre-compute the coarsened graphs based on their topological properties, while showing a comparable performance with respect to state-of-the-art *differentiable* pooling methods. The latter learn how to pool graphs end-to-end via gradient descent, at the cost of a larger model complexity and higher training time. In particular, a GNN equipped with differentiable pooling layers requires a training time that is an order of magnitude greater than a GNN with NDP operators. The efficiency of NDP brings a significant advantage when GNNs are deployed in real-world scenarios subject to computational constraints, like in embedded devices and sensor networks.

The paper is organized as follows: in Section II, we formalize the problem and introduce the needed nomenclature; in Section III, we describe the proposed method and derive theoretical results; related works are discussed in Section IV; in Section V, we report experimental results; finally, Section VI concludes the paper.

*fibi@norceresearch.no

F. M. Bianchi is with NORCE, The Norwegian Research Centre

D. Grattarola is with the Faculty of Informatics, Università della Svizzera italiana, Switzerland

L. Livi is with Dept.s. of Computer Science and Mathematics, University of Manitoba, Canada, and Dept. of Computer Science, University of Exeter, United Kingdom

C. Alippi is with Faculty of Informatics, Università della Svizzera italiana, Switzerland, and Dept. of Electronics, Information, and Bioengineering, Politecnico di Milano, Italy

II. PRELIMINARIES

Let $G = \{\mathcal{V}, \mathcal{E}\}$ be a simple graph with $|\mathcal{V}| = M$ nodes, characterized by a symmetric adjacency matrix $\mathbf{A} \in \mathbb{R}^{M \times M}$. Define as *graph signal* $\mathbf{X} \in \mathbb{R}^{M \times F}$ the graph node features $\in \mathbb{R}^F$ (the i -th row of \mathbf{X} contains the features of the i -th node).

Let $\mathbf{L} = \mathbf{I}_M - \mathbf{D}^{-1/2} \mathbf{A} \mathbf{D}^{-1/2}$ be the symmetrically normalized Laplacian of the graph, where \mathbf{D} is a diagonal degree matrix s.t. D_{ii} is the degree of node i . The Laplacian \mathbf{L} characterizes the dynamics of a diffusion process on the graph, and plays a fundamental role in the MP operations and the graph reduction procedure presented in the next Section.

For simplicity, we consider graphs with undirected and unweighted edges only, although the extension to directed edges or edges with attributes can be easily implemented by following Refs. [5], [6]. Likewise, graphs exposing self-loops require minor changes in the GNN, but do not affect NDP.

We consider a GNN composed of a stack of MP layers, each one followed by a graph pooling operation. The i -th pooling operation reduces M_{i-1} nodes to $M_i < M_{i-1}$, producing a pooled version of the node features $\mathbf{X}^{(i)} \in \mathbb{R}^{M_i \times F}$ and adjacency matrix $\mathbf{A}^{(i)} \in \mathbb{R}^{M_i \times M_i}$. As MP layer, we consider a simple formulation that operates on the first-order neighbourhood of each node and accounts for the original node features through a separate set of weights acting as a layer-wise skip connection. The computation carried out by the (j)-th MP layer can be expressed as

$$\begin{aligned} \mathbf{X}^{(j)} &= MP(\mathbf{X}^{(j-1)}, \mathbf{L}; \Theta_{MP}) \\ &= \text{ReLU}(\mathbf{L}\mathbf{X}^{(j-1)}\mathbf{W}_m + \mathbf{X}^{(j-1)}\mathbf{W}_s), \end{aligned} \quad (1)$$

where $\Theta_{MP} = \{\mathbf{W}_m, \mathbf{W}_s\}$ are the trainable weights relative to the mixing and skip component of the layer, respectively. Several other types of MP (e.g., [7], [8], [9], [10], [11], [12]) can also be used without affecting how NDP works.

III. PROPOSED GRAPH POOLING METHOD

In the following, we describe the proposed NDP operation that consists of three steps, depicted in Fig. 1: (A) decimate the nodes by dropping one of the two sides of the MAXCUT partition, (B) connect the remaining nodes with a *link construction* procedure, (C) sparsify the resulting graph to keep only those edges whose entry in the Laplacian is above a given threshold (i.e., *strong* connections with high weight). The proposed method is completely unsupervised as both the coarsened graphs and the nodes to be pooled are defined in a pre-processing step, before training the GNN.

A. Node decimation with MAXCUT spectral partitioning

Similarly to pooling operations in Convolutional Neural Networks (CNNs), which compute local summaries of neighboring pixels, we propose a pooling procedure that provides an effective coverage of the whole graph and reduces the number of nodes approximately by a factor of 2 (the usual reduction factor in CNN pooling). This can be achieved by partitioning the nodes in two sets, so that the nodes in one set are (strongly) connected to the nodes on the other side

of the partition, and then dropping one of the two sets. The reason is that (strongly) connected nodes exchange a lot of information after a MP operation and, as a result, their features become similar. Therefore, one set alone can represent the whole graph sufficiently well. This is similar to pooling in CNNs, where the maximum or the average is extracted from a small patch of neighboring pixels, which are assumed to be highly correlated and to contain similar information. In the following, we formalize the problem of finding the optimal subset of vertices that can be used to represent the whole graph.

The partition of the vertices (a cut) that maximizes the weight of the edges (volume) whose endpoints are on different sides of the partition is the solution of the MAXCUT problem [13]. The MAXCUT objective is expressed by the integer quadratic problem

$$\max \sum_{(i,j) \in \mathcal{E}} a_{i,j}(1 - z_i z_j) \quad \text{s.t. } z_i \in \{-1, 1\}, \forall i \in \mathcal{V} \quad (2)$$

where z_i indicates to which side of the partition node i is assigned to. Problem (2) is NP-hard and heuristics are considered in order to solve it. The heuristic that gives the best-known approximate MAXCUT solution in polynomial time is the Goemans-Williamson algorithm, which is based on the Semi-Definite Programming (SDP) relaxation [14]. Solving SDP is cumbersome and requires specific optimization programs that scale poorly on large graphs. Therefore, here we propose a simpler approach that relies on spectral partitioning.

We elaborate the objective function in (2) as a quadratic form of the graph Laplacian:

$$\begin{aligned} \sum_{i,j} a_{i,j}(1 - z_i z_j) &= \sum_{i,j} a_{i,j} \left(\frac{z_i^2 + z_j^2}{2} - z_i z_j \right) \\ &= \frac{1}{2} \sum_i \left[\sum_j a_{i,j} \right] z_i^2 + \frac{1}{2} \sum_j \left[\sum_i a_{i,j} \right] z_j^2 - \sum_{i,j} a_{i,j} z_i z_j \\ &= \frac{1}{2} \sum_i d_{i,i} z_i^2 + \frac{1}{2} \sum_j d_{j,j} z_j^2 - \mathbf{z}^T \mathbf{A} \mathbf{z} \\ &= \mathbf{z}^T \mathbf{D} \mathbf{z} - \mathbf{z}^T \mathbf{A} \mathbf{z} = \mathbf{z}^T \mathbf{L} \mathbf{z}. \end{aligned}$$

Then, we consider a continuous relaxation of the integer problem (2), by letting the discrete cluster assignment vectors to assume the continuous values \mathbf{c} :

$$\max \mathbf{c}^T \mathbf{L} \mathbf{c}, \quad \text{s.t. } \mathbf{c} \in \mathbb{R}^M \quad \text{and} \quad \|\mathbf{c}\|^2 = 1. \quad (3)$$

Eq. 3 can be solved by considering the Lagrange multiplier $\mathbf{c}^T \mathbf{L} \mathbf{c} + \lambda \mathbf{c}^T \mathbf{c}$ to find the maximum of $\mathbf{c}^T \mathbf{L} \mathbf{c}$ with the additional constraint $\|\mathbf{c}\|^2 = 1$. By setting to zero the derivative of the Lagrange multiplier, we recover the eigenvalue equation $\mathbf{L} \mathbf{c} + \lambda \mathbf{c} = 0$. Since all eigenvalues of \mathbf{L} are non-negative, by restricting the space of feasible solutions to vectors of unitary norm, the trivial solution $\mathbf{c}^* = \infty$ is excluded. In particular, if $\|\mathbf{c}\|^2 = 1$, then $\mathbf{c}^T \mathbf{L} \mathbf{c}$ is a Rayleigh quotient that reaches its maximum λ_{\max} (the largest eigenvalue of \mathbf{L}) when \mathbf{c}^* is the eigenvector \mathbf{v}_{\max} associated to λ_{\max} .

Since the values in \mathbf{v}_{\max} span the whole $[-1, 1]$ interval, we need to find a discrete solution \mathbf{z} for the MAXCUT problem. We can find an optimal cut $\mathbf{z}^* \in \mathcal{Z}$, where $\mathcal{Z} = \{\mathbf{z} : \mathbf{z} \in$

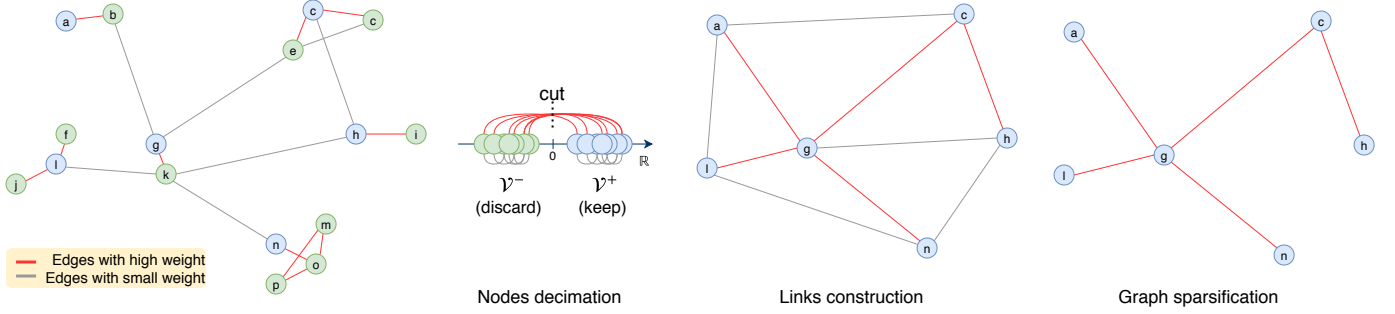


Fig. 1. High-level representation of the proposed graph coarsening procedure. First, nodes are partitioned in two sets according to a MAXCUT objective, and the decimated by dropping one of the two sets (\mathcal{V}^-). Then, a coarsened graph is built by connecting the remaining nodes with a graph reduction procedure. Finally, the edges with low weights are dropped to make the resulting graph sparse.

$\{-1, 1\}^M$ is the set of all feasible cuts, so that \mathbf{z}^* is the closest cut to \mathbf{c}^* . This amounts to solving the problem

$$\mathbf{z}^* = \arg \min \{\|\mathbf{c}^* - \mathbf{z}\| : \mathbf{z} \in \mathcal{Z}\}, \quad (4)$$

with the optimum given by

$$z_i^* = \begin{cases} 1, & c_i^* \geq 0, \\ -1, & c_i^* < 0. \end{cases} \quad (5)$$

Given the above rounding procedure, we partition the nodes among \mathcal{V}^+ and $\mathcal{V}^- = \mathcal{V} \setminus \mathcal{V}^+$ according to the rule

$$\mathcal{V}^+ = \{i \in \mathcal{V} : \mathbf{v}_{\max}(i) \geq 0\}. \quad (6)$$

The node decimation procedure offers two important advantages: i) it removes approximately half of the nodes, i.e., $|\mathcal{V}^+| \approx |\mathcal{V}^-|$; ii) \mathbf{v}_{\max} can be quickly computed with the power method [15]. The proposed method based on spectral partitioning finds the optimal MAXCUT if the graph is bipartite and yields good partitions if the graph is close to be bipartite, since the positive and negative values in \mathbf{v}_{\max} are grouped in two compact and separated clusters. If the structure of the graph is far from being bipartite, e.g., the connections are distributed uniformly and have similar weights, most of the values in \mathbf{v}_{\max} are concentrated around zero and it is difficult to accurately partition the vertices. However, in those cases the optimal MAXCUT solution is not much larger than the one given by a random cut¹ and, therefore, imprecision in the vertex assignments has a negligible effect on the solution. Intuitively, if all vertices are uniformly connected, they will carry similar information after an MP operation, hence, sampling them uniformly is an acceptable solution.

There is a strong analogy between the proposed spectral partitioning and spectral clustering [16]. However, a fundamental difference is that spectral clustering optimizes a minCUT rather than a MAXCUT objective [17], [18]. In other words, spectral clustering tries to isolate two or more clusters of densely connected nodes by cutting edges with small weights, while we cut edges with high weights yielding two sets of nodes, \mathcal{V}^+ and \mathcal{V}^- , that cover the original graph in a similar way.

¹a random cut \mathbf{z} is, in average, at least 0.5 of the optimal cut \mathbf{z}^* : $\mathbb{E}[\|\mathbf{z}\|] = \sum_{(i,j) \in \mathcal{E}} \mathbb{E}[z_i z_j] = \sum_{(i,j) \in \mathcal{E}} \Pr[(i,j) \in \mathbf{z}] = \frac{|\mathcal{E}|}{2} \geq \frac{\|\mathbf{z}^*\|}{2}$.

To decimate the nodes in NDP, we always drop the set of nodes in \mathcal{V}^- , i.e. the nodes associated with a negative value in \mathbf{v}_{\max} ; dropping the nodes in \mathcal{V}^+ would be equivalent.

From this analysis, it follows that the largest eigenvalue λ_{\max} is an upper bound for the MAXCUT problem. In our framework, the proposed partitioning scheme offers a good compromise between the accuracy of the cut, the simplicity of the algorithm, and the low computational complexity. We acknowledge other works that, with more complex spectral methods, obtain narrower bounds on the optimality of the MAXCUT solution [19], [20], [21]. However, such methods are too complex to be used in GNNs.

B. Links construction on the coarsened graph

After dropping the nodes in \mathcal{V}^- and all their incident edges, the resulting graph is usually disconnected. As a consequence, the ensuing MP operations become ineffective, since the features of disjoint subgraphs cannot be combined. Therefore, we build a Laplacian matrix that connects the remaining nodes in \mathcal{V}^+ using a link construction procedure. In particular, we consider the Kron reduction [22], which computes the reduced Laplacian as

$$\mathbf{L}^{\text{pool}} = \mathbf{L}_{\mathcal{V}^+, \mathcal{V}^+} - \mathbf{L}_{\mathcal{V}^+, \mathcal{V}^-} \mathbf{L}_{\mathcal{V}^-, \mathcal{V}^-}^{-1} \mathbf{L}_{\mathcal{V}^-, \mathcal{V}^+} \quad (7)$$

where $\mathbf{L}_{\mathcal{V}^+, \mathcal{V}^-}$ identifies a sub-matrix of \mathbf{L} with rows (columns) corresponding to the nodes in \mathcal{V}^+ (\mathcal{V}^-). The resulting \mathbf{L}^{pool} is a well-defined Laplacian where two nodes are connected if and only if there is a path between them in the original \mathbf{L} . Also, \mathbf{L}^{pool} does not introduce self-loops and guarantees the preservation of resistance distance [4]. Finally, Kron reduction guarantees spectral interlacing between the original Laplacian $\mathbf{L} \in \mathbb{R}^{M \times M}$ and the new coarsened one $\mathbf{L}^{\text{pool}} \in \mathbb{R}^{M^{\text{pool}} \times M^{\text{pool}}}$, with $M^{\text{pool}} < M$, i.e., given the spectrum Λ^{pool} of \mathbf{L}^{pool} and the spectrum Λ of \mathbf{L} , we have $\lambda_i \geq \lambda_i^{\text{pool}} \geq \lambda_{M-M^{\text{pool}}+i}$, $\forall i = 1, \dots, M^{\text{pool}}$, $\lambda_i \in \Lambda$, and $\lambda_i^{\text{pool}} \in \Lambda^{\text{pool}}$.

C. Graph sparsification

Due to the connectivity preservation property, by repeatedly applying Kron reduction the coarsened graphs become denser and their connectivity less localized. This implies a higher computational burden in deeper layers of the network, since the complexity of MP operations scales with the number of

edges. A possible solution would be to apply the spectral sparsification algorithm proposed in [23] on \mathbf{L}^{pool} , however, we empirically found that it leads to numerical instability and poor convergence during the learning phase.

Therefore, to limit the growth of non-zero entries after each reduction step, we propose a sparsification procedure that drops in the coarsened graph the connections whose entry in the Laplacian is below a small, user-defined threshold ϵ . In the following, we prove that, when using the proposed technique, the spectrum of the coarsened Laplacian is preserved up to a small factor that depends on ϵ .

Theorem 1. *Let \mathbf{Q} be a matrix used to remove small values in the Laplacian \mathbf{L} , which is defined as*

$$\mathbf{Q} = \begin{cases} Q_{i,j} = -L_{i,j}, & \text{if } |L_{i,j}| \leq \epsilon \\ Q_{i,j} = 0, & \text{otherwise.} \end{cases}$$

Each eigenvalue $\bar{\lambda}_i$ of the sparsified Laplacian $\bar{\mathbf{L}} = \mathbf{L} + \mathbf{Q}$ is bounded by

$$\bar{\lambda}_i \leq \lambda_i + \frac{\mathbf{v}_i^T \mathbf{Q} \mathbf{v}_i}{\mathbf{v}_i^T \mathbf{v}_i},$$

where λ_i and \mathbf{v}_i are eigenvalue-eigenvector pairs of \mathbf{L} .

Proof. Let \mathbf{P} be a matrix with elements $P_{i,j} = \text{sign}(Q_{i,j})$ and consider the perturbation $\mathbf{L} + \epsilon \mathbf{P}$, which modifies the eigenvalue problem $\mathbf{L} \mathbf{v}_i = \lambda_i \mathbf{v}_i$ in

$$(\mathbf{L} + \epsilon \mathbf{P})(\mathbf{v}_i + \mathbf{v}_\epsilon) = (\lambda_i + \lambda_\epsilon)(\mathbf{v}_i + \mathbf{v}_\epsilon). \quad (8)$$

where λ_ϵ and \mathbf{v}_ϵ are small perturbations on the eigenvalues and eigenvectors, respectively, to be estimated. By expanding (8), then canceling the equation $\mathbf{L} \mathbf{v}_i = \lambda_i \mathbf{v}_i$ and the high order terms $\mathcal{O}(\epsilon^2)$, one obtains

$$\mathbf{L} \mathbf{v}_\epsilon + \epsilon \mathbf{P} \mathbf{v}_i = \lambda_i \mathbf{v}_\epsilon + \lambda_\epsilon \mathbf{v}_i. \quad (9)$$

Since \mathbf{L} is symmetric, its eigenvectors can be used as a basis to express the perturbed eigenvectors

$$\mathbf{v}_\epsilon = \sum_{j=1}^N \delta_{ij} \mathbf{v}_j, \quad (10)$$

where δ_{ij} are (small) unknown coefficients. Substituting (10) in (9) and bringing \mathbf{L} inside the sum, gives

$$\sum_{j=1}^N \delta_{ij} \mathbf{L} \mathbf{v}_j + \epsilon \mathbf{P} \mathbf{v}_i = \lambda_i \sum_{j=1}^N \delta_{ij} \mathbf{v}_j + \lambda_\epsilon \mathbf{v}_i. \quad (11)$$

By considering the original eigenvalue problem that gives $\sum_{j=1}^N \delta_{ij} \mathbf{L} \mathbf{v}_j = \sum_{j=1}^N \delta_{ij} \lambda_j \mathbf{v}_j$ and by left-multiplying each term with \mathbf{v}_i^T , (11) becomes

$$\mathbf{v}_i^T \sum_{j=1}^N \delta_{ij} \lambda_j \mathbf{v}_j + \mathbf{v}_i^T \epsilon \mathbf{P} \mathbf{v}_i = \mathbf{v}_i^T \lambda_i \sum_{j=1}^N \delta_{ij} \mathbf{v}_j + \mathbf{v}_i^T \lambda_\epsilon \mathbf{v}_i. \quad (12)$$

Since eigenvectors are orthogonal, $\mathbf{v}_i^T \mathbf{v}_j = 0, \forall j \neq i$, Eq. (12) becomes

$$\begin{aligned} \mathbf{v}_i^T \delta_{ii} \lambda_i \mathbf{v}_i + \mathbf{v}_i^T \epsilon \mathbf{P} \mathbf{v}_i &= \mathbf{v}_i^T \lambda_i \delta_{ii} \mathbf{v}_i + \mathbf{v}_i^T \lambda_i \mathbf{v}_i \rightarrow \mathbf{v}_i^T \epsilon \mathbf{P} \mathbf{v}_i \\ &= \mathbf{v}_i^T \lambda_\epsilon \mathbf{v}_i, \end{aligned}$$

which, in turn, gives

$$\lambda_\epsilon = \frac{\mathbf{v}_i^T \epsilon \mathbf{P} \mathbf{v}_i}{\mathbf{v}_i^T \mathbf{v}_i} \geq \frac{\mathbf{v}_i^T \mathbf{Q} \mathbf{v}_i}{\mathbf{v}_i^T \mathbf{v}_i},$$

as $\mathbf{Q} \leq \epsilon \mathbf{P}$. \square

1) *Example:* Fig. 2 shows that the original spectrum $\Lambda(\mathbf{L}^0)$ is well-preserved in the coarsened Laplacians \mathbf{L}^1 , \mathbf{L}^2 , and \mathbf{L}^3 , after applying three consecutive Kron reductions followed by the proposed sparsification operation with a small ϵ (in this example, and in all other experiments in this paper, $\epsilon = 10^{-4}$).

Fig. 3 shows the edges in the original graph, with Laplacian \mathbf{L}^0 , and those obtained after Kron reduction. Fig. 4, instead, shows the remaining edges when the proposed sparsification method is applied. Given that the cost of a MP operation scales with the number of edges, thanks to the proposed sparsification procedure it is possible to greatly reduce the computation time in deeper layers of the GNN, without significantly altering the original graph spectra.

D. Pooling with decimation matrices.

To implement the reduction of node features as a differentiable operation to be used during training, we multiply the graph signal \mathbf{X} with a *decimation matrix* \mathbf{S} . The decimation matrix is obtained by keeping in the identity matrix \mathbf{I}_M only the rows corresponding to the vertices in \mathcal{V}^+ ,

$$\mathbf{X}^{\text{pool}} = \mathbf{S} \mathbf{X} = [\mathbf{I}_M]_{\mathcal{V}^+, \mathcal{V}} \mathbf{X}. \quad (13)$$

The application of a single decimation matrix $\mathbf{S}^{(i)}$ corresponds to a classic pooling with stride 2, since each graph reduction approximately halves the number of nodes. However, pooling with a stride $\approx 2^k$ can be obtained by applying k decimation matrices in cascade. This corresponds to going from level i to level $i+k$ ($k > 1$) in the pyramid of coarsened graphs. Fig. 5 shows an example of pooling with stride 8, which allows to apply a MP layer using Laplacian $\mathbf{L}^{(3)}$ after the MP operation on $\mathbf{L}^{(0)}$.

IV. RELATED WORK

In this section, we discuss related works, distinguishing between *topological* and *differentiable* pooling methods.

a) *Topological pooling methods:* similarly to NDP, topological pooling methods account only for the graph topology and pre-compute the coarsened graphs before training. Topological pooling methods are usually unsupervised, as they define how to coarsen the graph outside of the learning procedure. The GNN is then trained to fit its graph representation to these pre-determined structures. Pre-computing graph coarsening not only makes the training much faster by avoiding graph reduction at every forward pass in the GNN, but also provides a strong inductive bias that prevents degenerate solutions, such as entire graphs being collapsed into a single node or important parts of a graph being discarded. This is important when dealing with small datasets or, as it will be discussed later, in tasks such as graph signal classification.

The approach that is most related to our work, and that has been adopted by several GNN architectures to perform

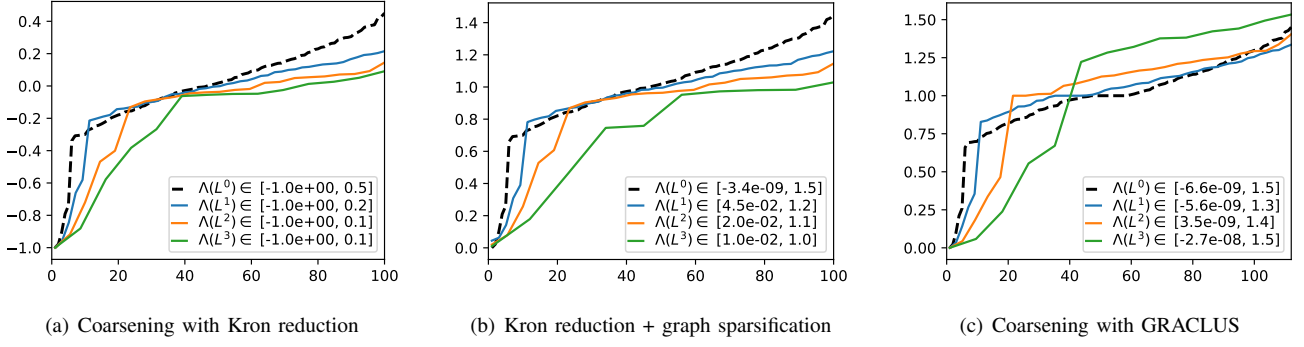


Fig. 2. Spectrum of the original Laplacian, $\Lambda(\mathbf{L}^0)$, and of the reduced Laplacians after n applications of graph coarsening $\Lambda(\mathbf{L}^n)$. Fig (a) shows how Kron reduction preserves spectral interlacing. Fig (b) shows that spectral interlacing is maintained even after applying the proposed sparsification. Fig (c) shows that coarsening the graph with GRACLUS [24] gives spectra that are not interlaced anymore.

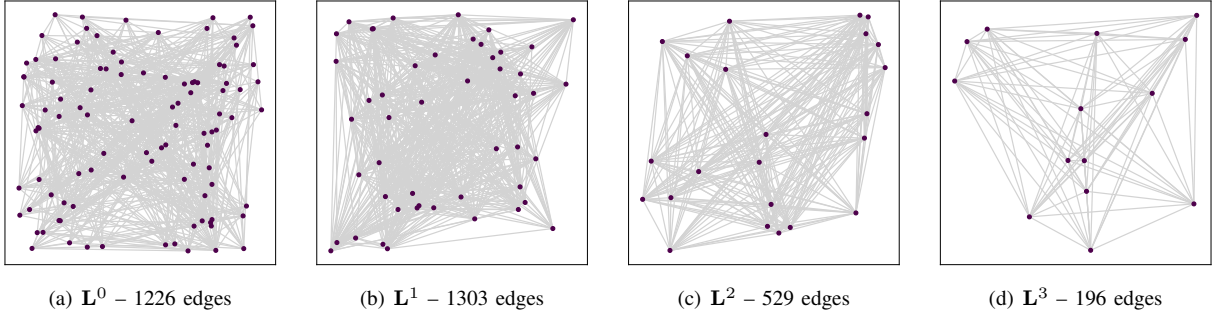


Fig. 3. Laplacians coarsened with Kron reduction.

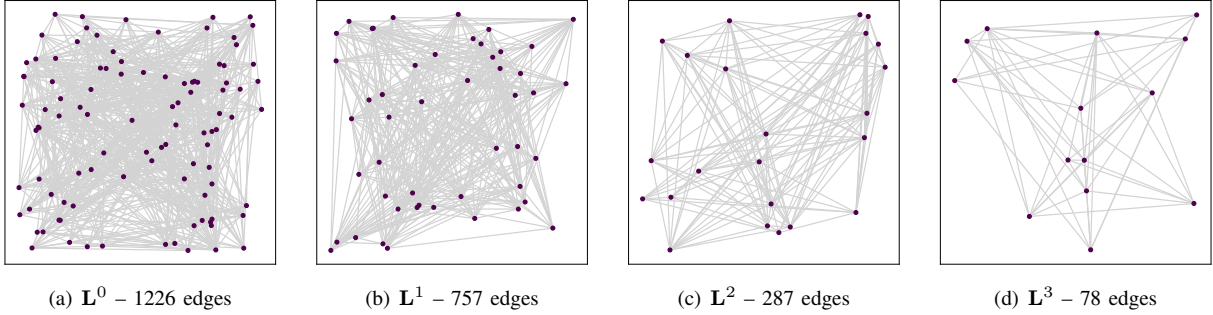


Fig. 4. Laplacians coarsened with Kron reduction and sparsified with the proposed sparsification method.

pooling [25], [7], [26], [27], [28], consists of coarsening the graph with GRACLUS, a hierarchical spectral clustering algorithm [24]. At each level l , two vertices $x_i^{(l)}$ and $x_j^{(l)}$ are clustered together in a new vertex $x_z^{(l+1)}$. Then, a standard pooling operation (like average or max) is applied to halve the size of the graph signal. To make the pooling output consistent with the cluster assignment, the rows of graph signal \mathbf{X} are rearranged so that nodes i and j end up in consecutive positions. This approach has several drawbacks. First, the connectivity of the original graph is not preserved in the coarsened graphs and the spectrum of their associated Laplacians is usually not contained in the spectrum of the original Laplacian (see Fig. 2(c)). Second, the procedure to rearrange vertices is cumbersome to implement. Moreover, GRACLUS pooling requires to add fake vertices so that the number of nodes can

be halved each time. This not only injects noisy information in the graph signal, but also introduces additional nodes with a consequent increment of the computational time in the GNN, both in training and evaluation. Finally, the clustering depends on the initial ordering of the nodes, which hampers stability and reproducibility.

NDP addresses the drawbacks of GRACLUS pooling since it does not require to introduce fake nodes and to reorder them according to their cluster indices. Additionally, the outcome of NDP does not depend on the node ordering and the coarsened graphs preserve the original connectivity and spectrum.

An alternative approach to spectral clustering is to directly cluster the rows (or the columns) of the adjacency matrix. A representative of this strategy is the pooling approach proposed in [29], which decomposes the adjacency matrix using the Non-

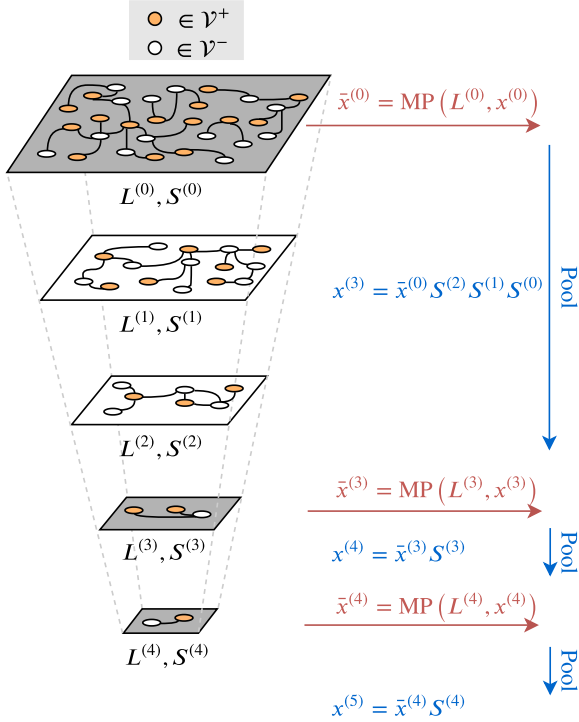


Fig. 5. Example of higher-order graph pooling. After the first MP operation, the graph is reduced by repeatedly applying NDP until the desired graph size is reached. The node features are pooled by applying in cascade multiple decimation matrices.

negative Matrix Factorization (NMF) $\mathbf{A} \approx \mathbf{W}\mathbf{H}$. The NMF has the inherent property of automatically clustering the columns of the input matrix and it can be shown that the minimization of the NMF objective is mathematically equivalent to the minimization in k -means clustering [30]. In particular, $\mathbf{W} \in \mathbb{R}^{N \times K}$ is interpreted as the cluster representatives matrix and $\mathbf{H} \in \mathbb{R}^{K \times N}$ as a soft-cluster assignment matrix of the columns in \mathbf{A} . Therefore, the pooled node features and the coarsened graph can be obtained as $\mathbf{X}^{\text{pool}} = \mathbf{H}^T \mathbf{X}$ and $\mathbf{A}^{\text{pool}} = \mathbf{H}^T \mathbf{X} \mathbf{H}$, respectively. The main drawback of this approach is that NMF does not scale well to large graphs.

A pooling operation to coarsen binary unweighted graphs by aggregating maximal cliques is proposed in [31]. Nodes assigned to the same clique are summarized by max or average pooling and become a new node in the coarsened graph. If a node in one clique shares an edge with a node in another, the nodes representing the cliques are connected in the new graph. A disadvantage of this method is the computational complexity in finding the cliques.

b) Differentiable pooling methods: these methods learn how to generate a coarsened version of the graph through differentiable functions, which are parametrized by weights that are optimized for the task at hand, and as such are usually supervised. Differently from topological pooling, the differentiable methods usually take the node features as input and evolve as the GNN is trained. While this gives more flexibility in learning the optimal representations for a specific task, GNNs with differentiable pooling have more parameters

and hence are prone to overfitting.

DiffPool [32] is a pooling method that learns differentiable soft assignments to cluster the nodes at each layer. DiffPool uses two MP layers in parallel: one to update the node features, and one to generate the cluster assignments. The original adjacency matrix acts as a prior when learning the soft assignments, and sparsity in the cluster assignments is enforced with an entropy-based regularization. The application of this method to large graphs is not practical, as the size of the cluster assignment matrix is quadratic in the number of nodes.

A second approach, dubbed *Top-K* pooling [33], [34], learns a projection vector that is applied to each node feature to obtain a score. The nodes with the K highest scores are then retained, while the remaining ones are dropped. Since the top- K selection is not differentiable, the scores are also used as a gating for the node features, allowing gradients to flow through the projection vector during backpropagation. Top- K is more memory efficient than DiffPool as it avoids generating cluster assignments. To prevent the adjacency matrix \mathbf{A} from becoming disconnected when the nodes are removed, Top- K drops rows and columns from \mathbf{A}^2 , and uses it as the new adjacency matrix. However, computing \mathbf{A}^2 has a cost of $\mathcal{O}(N^2)$ and it is inefficient to implement even with sparse operations. A variant proposed in [35] introduces in Top- K pooling a soft attention mechanism for selecting the nodes to retain.

Another differentiable pooling method proposed in [36] selects the nodes with the highest variations within their neighborhood (local peaks on the graph signal) as cluster representatives. Then, the graphs are coarsened and the node features are pooled by assigning the remaining nodes to their representative. Pooling by Edge Contraction [37], [38] iteratively contracts edges (i.e., merges their endpoints) according to a score learned by a small network fed with the features of the two end nodes. When two nodes are merged, the new node inherits all the edges incident to the two original nodes. Finally, a pooling procedure proposed in [39] diffuses a signal from designated nodes on the graph and stores the observed sequence of diffused components. The resulting stream of information is interpreted as a time signal, where standard pooling techniques are applied.

V. EXPERIMENTS

We consider two main tasks on graph-structured data: graph classification and graph signal classification. The code for all the experiments is based on Spektral², a Python library for GNNs, and the code to replicate all experiments of this paper is publicly available on GitHub³.

A. Graph classification

In this task, the i -th sample is a graph represented by a pair $\{\mathbf{A}_i, \mathbf{X}_i\}$, $i = 1, \dots, N$, where $\mathbf{A}_i \in \mathbb{R}^{M_i \times M_i}$ is an adjacency matrix with M_i nodes, and $\mathbf{X}_i \in \mathbb{R}^{M_i \times F}$ encodes node features. Each sample must be classified with a label y_i .

²<https://github.com/danielegrattarola/spektral>

³github.com/danielegrattarola/decimation-pooling

We consider two datasets of synthetic graphs⁴ (*Bench-easy* and *Bench-hard*) and eight dataset of real-world graphs from the benchmark database for graph kernels⁵: *Proteins*, *Enzymes*, *NCII*, *MUTAG*, *Mutagenicity*, *D&D*, *COLLAB*, and *Reddit-Binary*. When node features are not available, we use node degrees and clustering coefficients as surrogate node features. Moreover, we use node labels as additional node features whenever they are available.

In the following, we compare NDP with DiffPool [32], Top- K [33], GRACLU [7], and NMF [29]. In each experiment we adopt a fixed network architecture, MP(32)-P(2)-MP(32)-P(2)-MP(32)-AvgPool-Softmax, where MP(32) stands for a MP layer as described in (1) configured with 32 hidden units and ReLU activations, P(2) is a pooling operation with stride 2, AvgPool is a global average pooling operation on all the remaining graph nodes, and Softmax indicates a fully connected layer with Softmax activation. As training algorithm, we use Adam [40] with initial learning rate $5e-4$ and L_2 regularization with weight $1e-4$.

As additional baselines, we consider the popular Weisfeiler-Lehman (WL) graph kernel [41], resulting in a GNN with only MP layers (*Flat*), and a network with only fully connected layers (*Dense*). The comparison with *Flat* helps to understand whether pooling operations are useful for a given task. The results obtained by *Dense*, instead, help to quantify how much additional information is brought by the graph structure compared to considering the node features alone. To train the GNN on mini-batches of graphs with a variable number of nodes, we build the disjoint union of the graphs in each mini-batch and train the GNN on the combined Laplacian and graph signal. In this way, it is possible to apply MP and pooling operations without resorting to zero-padding. Fig. 6 reports an example of the adopted procedure.

We evaluate the model performance by splitting the dataset in 10 groups. Each unique group is, in turn, selected as the test set, while the remaining 9 groups become the training set. Each time we consider a different train/test split, we set aside 10% of the training data as validation set, which is only used to compute early stopping (we interrupt the training procedure after the loss on the validation set does not decrease for 50 epochs).

We report in Table I the test accuracy averaged over the 10 folds. We note that no single architecture outperforms every other in all tasks. The WL kernel achieves the best results on NCII and Mutagenicity, but it does not perform well on the other datasets. Surprisingly, the *Dense* architecture achieves the best performance on MUTAG, indicating that in this case, the connectivity of the graphs does not carry useful information for the classification task. The performance of the *Flat* baseline indicates that, in Enzymes and COLLAB, pooling operations are not useful to improve the classification accuracy.

NDP consistently achieves a higher accuracy compared to GRACLU and NMF, which are topological pooling methods as well. The main reason for the lower performance of GRACLU is the injection of fake nodes in the graph,

which introduce noise in the data samples. Among the two differentiable pooling methods, DiffPool always outperforms Top- K . The reason is that Top- K tends to discard large parts of the graphs, thus ignoring important information that is necessary to perform classification.

In Fig. 7, we report the training time for the five different pooling methods. As expected, GNNs configured with GRACLU, NMF, and NDP are much faster to train compared to those based on DiffPool and Top- K , with NDP being slightly faster than the other two topological methods. Top- K is generally slower than DiffPool due to the costly computation of A^2 at every forward pass. In Fig. 8, we plot the average training time per epoch against the average accuracy obtained by each pooling method on the ten graph classification tasks taken into account. The scatter plot is obtained from the data reported in Tab. I and Fig. 7. On average, NDP obtains the highest classification accuracy, slightly outperforming even DiffPool, while being, at the same time, the fastest among all pooling methods.

To better understand the differences in computing time and, in general, the behavior of the topological pooling methods under analysis, we randomly selected one graph from the Enzymes dataset and report in Fig. 9 the coarsened Laplacians computed by GRACLU, NMF, and NDP. Fig. 9(a) shows the original graph, while in (b), (c), and (d), the first column depicts the non-zero entries of the first Laplacian $L^{(0)}$, and the second and third columns depict the Laplacian after the first ($L^{(1)}$) and second pooling operation ($L^{(2)}$), respectively. From Fig. 9(b) we notice that the first Laplacian $L^{(0)}$ used in GRACLU has a higher number of nodes than the original graph (48, against the original 39 nodes), and has also a different structure. As discussed in Sect. IV, GRACLU adds fake nodes to the graph, so that they can be exactly halved at every pooling operation. Also, it reorders the nodes such that the two nodes to be pooled together end up in consecutive positions. Fig. 9(c) shows that NMF produces graphs that are very dense or even fully connected. This is a consequence of a multiplication with the dense soft-assignment matrix in the construction of the coarsened graph. Finally, Fig. 9(d) shows that NDP produces coarsened Laplacians that are significantly more sparse than the ones computed by GRACLU and NMF. This is the key factor explaining the observed differences in computing time.

B. Graph signal classification

In this task, N different graph signals $\mathbf{X} \in \mathbb{R}^{M \times F_{in}}$, defined on the same adjacency matrix $\mathbf{A} \in \mathbb{R}^{M \times M}$, must be classified with labels $\mathbf{y}_1, \dots, \mathbf{y}_N$. We use the same architecture adopted for graph classification, with the only difference that each pooling operation is implemented with stride 4: MP(32)-P(4)-MP(32)-P(4)-MP(32)-AvgPool-Softmax. When using NDP a stride of 4 is obtained by applying two decimation matrices in cascade, $\mathbf{S}^{(1)}\mathbf{S}^{(0)}$ and $\mathbf{S}^{(3)}\mathbf{S}^{(2)}$, as discussed in Section III-D.

In the following, we report two experiments on graph signal classification: image classification on an 8-NN graph with MNIST and sentiment analysis on the IMDB dataset.

MNIST. For this experiment, we follow the same settings described in [7]. To emulate a classic CNNs operating on a

⁴https://github.com/FilippoMB/Benchmark_dataset_for_graph_classification

⁵<https://ls11-www.cs.tu-dortmund.de/staff/morris/graphkerneldatasets>

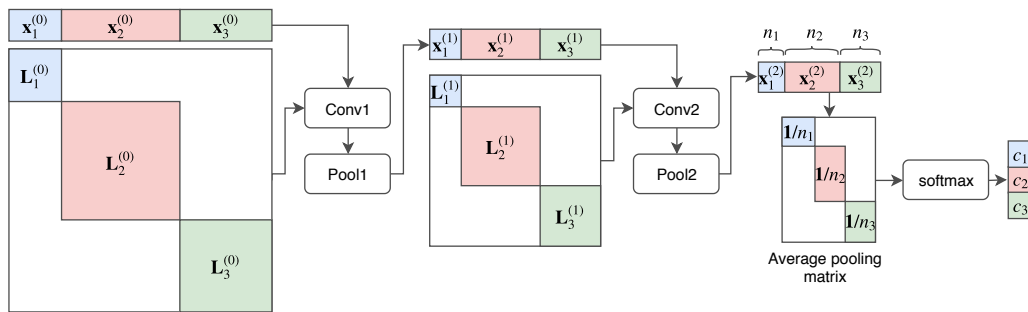


Fig. 6. Example of the implementation used in graph classification with mini-batches of size three.

TABLE I
GRAPH CLASSIFICATION ACCURACY. SIGNIFICANTLY BETTER RESULTS ($p < 0.05$) ARE IN BOLD.

Dataset	WL	Dense	Flat	Diffpool	Top- K	GRACLUS	NMF	NDP
Bench-easy	92.6	29.3 \pm 0.3	98.5 \pm 0.3	98.6 \pm 0.4	82.4 \pm 8.9	97.5 \pm 0.5	97.4 \pm 0.8	97.9 \pm 0.5
Bench-hard	60.0	29.4 \pm 0.3	67.6 \pm 2.8	69.9 \pm 1.9	42.7 \pm 15.2	69.0 \pm 1.5	68.6 \pm 1.6	72.6 \pm 0.9
Proteins	71.2 \pm 2.6	68.7 \pm 3.3	72.6 \pm 4.8	72.8 \pm 3.5	69.6 \pm 3.3	70.3 \pm 2.6	71.6 \pm 4.1	73.3 \pm 3.7
Enzymes	33.6 \pm 4.1	45.7 \pm 9.9	52.0 \pm 12.3	24.6 \pm 5.3	31.4 \pm 6.8	42.0 \pm 6.7	39.9 \pm 3.6	43.9 \pm 5.2
NCI1	81.1 \pm 1.6	53.7 \pm 3.0	74.4 \pm 2.5	76.5 \pm 2.2	71.8 \pm 2.6	69.5 \pm 1.7	68.2 \pm 2.2	73.5 \pm 1.90
MUTAG	78.9 \pm 13.1	91.1 \pm 7.1	87.1 \pm 6.6	90.5 \pm 3.9	85.5 \pm 11.0	82.9 \pm 6.5	76.7 \pm 14.4	84.7 \pm 7.4
Mutagenicity	81.7 \pm 1.1	68.4 \pm 0.3	78.0 \pm 1.3	77.6 \pm 2.7	71.9 \pm 3.7	74.4 \pm 1.8	75.5 \pm 1.7	78.1 \pm 2.0
D&D	78.6 \pm 2.7	70.6 \pm 5.2	76.8 \pm 1.5	79.3 \pm 2.4	69.4 \pm 7.8	70.5 \pm 4.8	70.6 \pm 4.1	72.0 \pm 3.1
COLLAB	74.8 \pm 1.3	79.3 \pm 1.6	82.1 \pm 1.8	81.8 \pm 1.4	79.3 \pm 1.8	77.1 \pm 2.1	78.5 \pm 1.8	79.1 \pm 1.5
Reddit-Binary	68.2 \pm 1.7	48.5 \pm 2.6	80.3 \pm 2.6	86.8 \pm 2.1	74.7 \pm 4.5	79.2 \pm 0.4	52.0 \pm 2.1	84.3 \pm 2.4

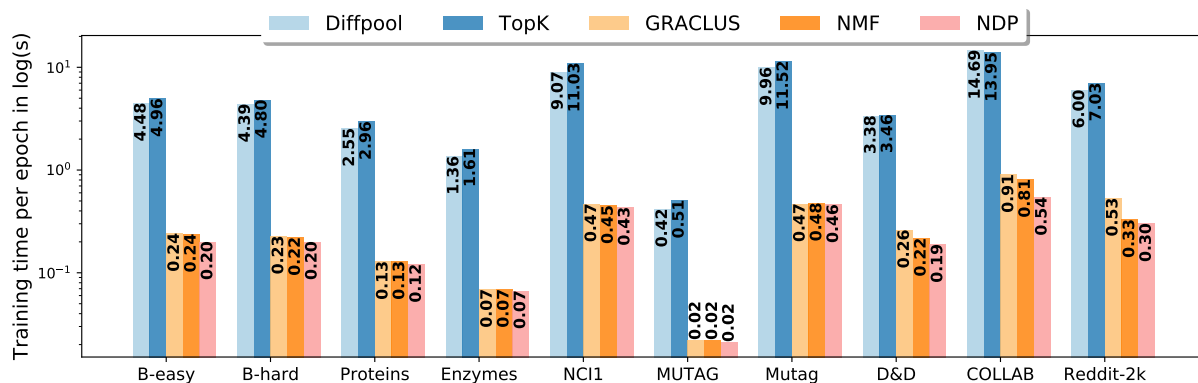


Fig. 7. Average training time per epoch (in seconds) for different pooling methods. The bars height is in logarithmic scale. Simulations were performed with an Nvidia GeForce GTX2080.

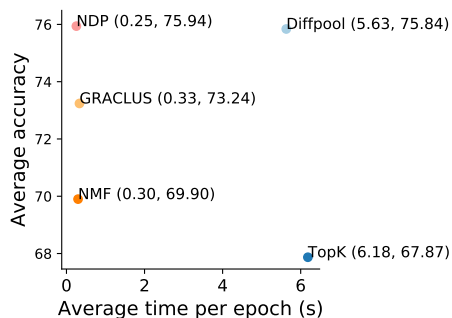


Fig. 8. Average training time per epoch against average accuracy, computed for each method over the 10 graph classification tasks.

regular 2D grid, an 8-NN graph is defined on the 784 pixels of the MNIST images, using the following similarity score between nodes:

$$a_{ij} = \exp\left(-\frac{\|p_i - p_j\|^2}{\sigma^2}\right), \quad (14)$$

where p_i and p_j are the 2D coordinates of pixel i and j . Each graph signal is a vectorized image $\mathbf{x} \in \mathbb{R}^{784 \times 1}$.

Tab. II reports the average results achieved over 10 independent runs by a GNN configured with the different pooling operations. Contrarily to what observed in graph classification, here, DiffPool and Top K do not seem to be suitable for solving this task, as they achieve an accuracy barely above random guessing. On the contrary, the three topological methods are able to obtain accuracy scores closer to the ones of classical

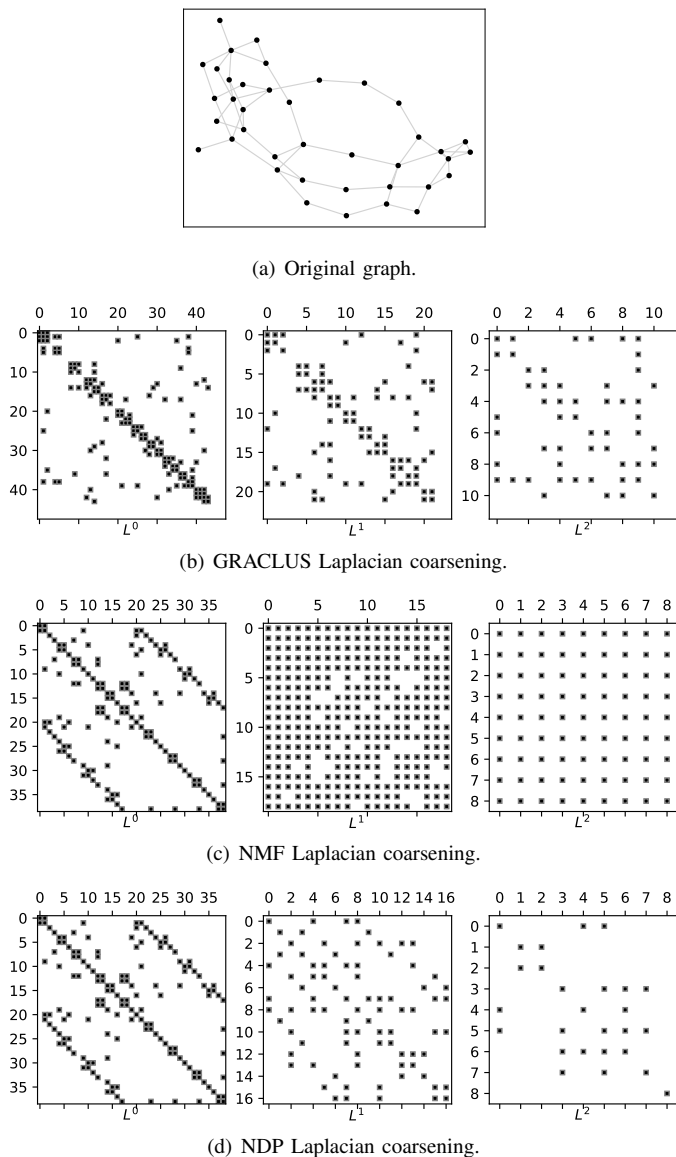


Fig. 9. Example of coarsening on one graph from the Enzymes dataset. In (a), the original adjacency matrix of the graph. In (b), (c), and (d) the edges of the Laplacians at coarsening level 0, 1, and 2, as obtained by the 3 different pooling methods GRACLUS, NMF, and the proposed NDP.

TABLE II
GRAPH SIGNAL CLASSIFICATION ACCURACY ON MNIST.

DiffPool	Top-K	GRACLUS	NMF	NDP
24.00 \pm 0.0	11.00 \pm 0.0	96.21 \pm 0.18	94.15 \pm 0.17	97.09 \pm 0.11

CNNs, with NDP significantly outperforming the other two techniques.

We argue that the poor performance of the two differentiable pooling methods is attributable to the low information content of the node features and the very homogeneous graph structure, due to the nodes having a constant number of edges and being connected only locally. This results in a graph with a very large diameter (maximum shortest path), where information

propagates slowly through MP layers. Therefore, even after MP, nodes in very different parts of the graph will end up having similar (if not identical) features, which leads them to be assigned to the same cluster. In turn, this makes the graph collapse and becomes densely connected, losing its original structure. On the other hand, topological pooling methods can preserve the graph structure by operating on the whole adjacency matrix at once to compute the coarsened graphs, and are not influenced by uninformative node features.

IMDB. In this task, we consider the IMDB sentiment analysis dataset of movies reviews, which must be classified as positive or negative. We use a graph that encodes the similarity of all words in the vocabulary. Each graph signal represents a review and consists of a binary vector with size equal to the vocabulary, which assumes value 1 in correspondence of a word that appears at least once in the review, and 0 otherwise.

The graph is built as follows. First, we extract a vocabulary from the most common words in the reviews. For each review, we consider at most 256 words, padding with a special token the reviews that are shorter and truncating those that are longer. Then, we train a simple classifier consisting of a word embedding layer [42] of size 200, followed by a dense layer with a ReLU activation, a dropout layer [43] with probability 0.5, and a dense layer with sigmoid activation. The classifier achieves a test accuracy of $\sim 85\%$. After training, we generate the word embedding for each word in the vocabulary and construct a 4-NN graph, according to the Euclidean similarity of the embedding vectors.

As baselines, we consider the classification accuracy obtained by a simple network used to generate the word embeddings (*Dense*) and two more advanced architectures. The first (*LSTM*), is a network where the dense hidden layer is replaced by a LSTM [44], which allows capturing the temporal dependencies in the sequence of words in the review. The other baseline (*TCN*) is a network where the hidden layers are 1D convolutions with different dilation rates [45]. In particular, we used a Temporal Convolution Network [46] with seven residual blocks with dilations [1, 2, 4, 8, 16, 32, 64], kernel size 6, causal padding, and dropout probability 0.3. The results averaged over 10 runs for vocabularies of different sizes (# Words) are reported in Tab. III.

Similarly to the MNIST experiment, we notice that neither DiffPool nor TopK are able to find effective solutions for this graph signal classification task. The reason can be once again attributed to the low information content of the individual node features and in the sparsity of the graph signal (most node features are 0), which make it difficult for the differentiable pooling methods to infer global properties of the graph by only looking at local sub-structures.

On the other hand, we observe that NDP consistently outperforms all baselines, including GRACLUS and NMF. We also note that the coarsened graphs generated by NMF when the vocabulary has 10k words are too dense to fit in the GPU memory⁶. Interestingly, the GNNs configured with GRACLUS and NDP always achieve better results than the *Dense* network, even if the latter generates the word embeddings used to build

⁶Simulations were performed with an Nvidia GeForce GTX2080.

TABLE III
GRAPH SIGNAL CLASSIFICATION ACCURACY ON IMDB SENTIMENT ANALYSIS DATASET.

# Words	Dense	LSTM	TCN	DiffPool	Top-K	GRACLUS	NMF	NDP
1k	82.65 \pm 0.01	86.58 \pm 0.03	85.61 \pm 0.14	50.00 \pm 0.0	50.00 \pm 0.0	85.03 \pm 0.10	82.51 \pm 0.11	87.75\pm0.03
5k	86.26 \pm 0.03	86.59 \pm 0.06	87.42 \pm 0.09	50.00 \pm 0.0	50.00 \pm 0.0	87.55 \pm 0.15	85.66 \pm 0.11	87.86\pm0.09
10k	83.75 \pm 0.02	85.98 \pm 0.04	87.38 \pm 0.07	50.00 \pm 0.0	50.00 \pm 0.0	87.29 \pm 0.07	OOM	87.78\pm0.04

the graph on which the GNN operates. This can be explained by the fact that the *Dense* network is able to immediately overfit the dataset, whereas introducing the graph structure imposes a strong regularization on the GNN, as words can only be combined with their neighbors on the vocabulary graph.

The *LSTM* baseline generally achieves a better accuracy than *Dense*, since it captures the sequential ordering of the words in the reviews, which also helps to prevent overfitting on training data. Finally, the *TCN* baseline always outperforms *LSTM*, both in terms of accuracy and computational costs. This substantiates recent findings showing that convolutional architectures may be more suitable than recurrent ones for tasks involving sequential data [46].

VI. CONCLUSIONS

In this paper, we proposed Node Decimation Pooling (NDP), a novel pooling strategy for Graph Neural Networks based on a spectral node decimation procedure. NDP works by partitioning a graph into two disjoint subsets of nodes, discarding one of the two sets, and finally connecting the nodes in the remaining set using Kron reduction. Because the node construction procedure yields graphs that are likely to be dense, we also introduced a graph sparsification technique to remove weak connections from the pooled graphs.

In addition, we formally showed a link between the spectral node decimation procedure on which NDP is based and the MAXCUT optimization problem. Finally, we also demonstrated that the graph sparsification procedure proposed in this work preserves the spectra of the pooled graph w.r.t. the original graph, up to an arbitrarily small constant.

We compared NDP with two main families of pooling methods for GNNs: topological (to which NDP belongs) and the state-of-the-art differentiable methods. NDP showed consistent advantages compared to both types of pooling. In particular, experimental results showed that NDP is less computationally expensive (in terms of both time and memory) than differentiable methods, by up to an order of magnitude. At the same time, NDP was able to achieve higher or competitive accuracy on all graph classification tasks taken into account. Finally, our results indicate that topological methods are the only viable approach for the graph signal classification tasks that we considered, with differentiable methods suffering a performance degradation, since they only operate locally on graphs.

REFERENCES

- [1] M. M. Bronstein, J. Bruna, Y. LeCun, A. Szlam, and P. Vandergheynst, "Geometric deep learning: Going beyond euclidean data," *IEEE Signal Processing Magazine*, vol. 34, no. 4, pp. 18–42, July 2017.
- [2] J. Gilmer, S. S. Schoenholz, P. F. Riley, O. Vinyals, and G. E. Dahl, "Neural message passing for quantum chemistry," in *Proceedings of the 34th International Conference on Machine Learning-Volume 70*. JMLR.org, 2017, pp. 1263–1272.
- [3] N. Tremblay, P. Goncalves, and P. Borgnat, "Design of graph filters and filterbanks," in *Cooperative and Graph Signal Processing*. Elsevier, 2018, pp. 299–324.
- [4] D. I. Shuman, M. J. Faraji, and P. Vandergheynst, "A multiscale pyramid transform for graph signals," *IEEE Transactions on Signal Processing*, vol. 64, no. 8, pp. 2119–2134, 2016.
- [5] M. Simonovsky and N. Komodakis, "Dynamic edge-conditioned filters in convolutional neural networks on graphs," in *Proceedings of the IEEE Conference on Computer Vision and Pattern Recognition*, 2017.
- [6] M. Schlichtkrull, T. N. Kipf, P. Bloem, R. Van Den Berg, I. Titov, and M. Welling, "Modeling relational data with graph convolutional networks," in *European Semantic Web Conference*. Springer, 2018, pp. 593–607.
- [7] M. Defferrard, X. Bresson, and P. Vandergheynst, "Convolutional neural networks on graphs with fast localized spectral filtering," in *Advances in Neural Information Processing Systems*, 2016, pp. 3844–3852.
- [8] T. N. Kipf and M. Welling, "Semi-supervised classification with graph convolutional networks," in *International Conference on Learning Representations (ICLR)*, 2016.
- [9] P. Velickovic, G. Cucurull, A. Casanova, A. Romero, P. Lio, and Y. Bengio, "Graph attention networks," *arXiv preprint arXiv:1710.10903*, 2017.
- [10] F. M. Bianchi, D. Grattarola, L. Livi, and C. Alippi, "Graph neural networks with convolutional arma filters," *arXiv preprint arXiv:1901.01343*, 2019.
- [11] K. Xu, W. Hu, J. Leskovec, and S. Jegelka, "How powerful are graph neural networks?" *arXiv preprint arXiv:1810.00826*, 2018.
- [12] W. Hamilton, Z. Ying, and J. Leskovec, "Inductive representation learning on large graphs," in *Advances in Neural Information Processing Systems*, 2017, pp. 1024–1034.
- [13] L. Palagi, V. Piccialli, F. Rendl, G. Rinaldi, and A. Wiegale, "Computational approaches to max-cut," in *Handbook on semidefinite, conic and polynomial optimization*. Springer, 2012, pp. 821–847.
- [14] M. X. Goemans and D. P. Williamson, "Improved approximation algorithms for maximum cut and satisfiability problems using semidefinite programming," *Journal of the ACM (JACM)*, vol. 42, no. 6, pp. 1115–1145, 1995.
- [15] F. M. Bianchi, E. Maiorino, L. Livi, A. Rizzi, and A. Sadeghian, "An agent-based algorithm exploiting multiple local dissimilarities for clusters mining and knowledge discovery," *Soft Computing*, vol. 21, no. 5, pp. 1347–1369, 2017.
- [16] U. Von Luxburg, "A tutorial on spectral clustering," *Statistics and computing*, vol. 17, no. 4, pp. 395–416, 2007.
- [17] J. Shi and J. Malik, "Normalized cuts and image segmentation," *Departmental Papers (CIS)*, p. 107, 2000.
- [18] F. M. Bianchi, D. Grattarola, and C. Alippi, "Mincut pooling in graph neural networks," *CoRR*, vol. abs/1907.00481, 2019.
- [19] S. Poljak and F. Rendl, "Solving the max-cut problem using eigenvalues," *Discrete Applied Mathematics*, vol. 62, no. 1-3, pp. 249–278, 1995.
- [20] J. A. Soto, "Improved analysis of a max-cut algorithm based on spectral partitioning," *SIAM Journal on Discrete Mathematics*, vol. 29, no. 1, pp. 259–268, 2015.
- [21] L. Trevisan, "Max cut and the smallest eigenvalue," *SIAM Journal on Computing*, vol. 41, no. 6, pp. 1769–1786, 2012.
- [22] F. Dorfler and F. Bullo, "Kron reduction of graphs with applications to electrical networks," *IEEE Transactions on Circuits and Systems I: Regular Papers*, vol. 60, no. 1, pp. 150–163, Jan 2013.
- [23] J. Batson, D. A. Spielman, N. Srivastava, and S.-H. Teng, "Spectral sparsification of graphs: theory and algorithms," *Communications of the ACM*, vol. 56, no. 8, pp. 87–94, 2013.

- [24] I. S. Dhillon, Y. Guan, and B. Kulis, "Kernel k-means: spectral clustering and normalized cuts," in *Proceedings of the tenth ACM SIGKDD international conference on Knowledge discovery and data mining*. ACM, 2004, pp. 551–556.
- [25] J. Bruna, W. Zaremba, A. Szlam, and Y. LeCun, "Spectral networks and locally connected networks on graphs," *arXiv preprint arXiv:1312.6203*, 2013.
- [26] F. Monti, D. Boscaini, J. Masci, E. Rodola, J. Svoboda, and M. M. Bronstein, "Geometric deep learning on graphs and manifolds using mixture model cnns," in *Proceedings of the IEEE Conference on Computer Vision and Pattern Recognition*, vol. 1, 2017, p. 3.
- [27] M. Fey, J. E. Lenssen, F. Weichert, and H. Müller, "Splinecnn: Fast geometric deep learning with continuous b-spline kernels," in *Proceedings of the IEEE Conference on Computer Vision and Pattern Recognition*, 2018, pp. 869–877.
- [28] R. Levie, F. Monti, X. Bresson, and M. M. Bronstein, "Cayleynets: Graph convolutional neural networks with complex rational spectral filters," *IEEE Transactions on Signal Processing*, vol. 67, no. 1, pp. 97–109, Jan 2019.
- [29] D. Bacciu and L. Di Sotto, "A non-negative factorization approach to node pooling in graph convolutional neural networks," in *Proceedings of the 18th International Conference of the Italian Association for Artificial Intelligence*. AIIA, 2019.
- [30] C. Ding, X. He, and H. D. Simon, "On the equivalence of nonnegative matrix factorization and spectral clustering," in *Proceedings of the 2005 SIAM International Conference on Data Mining*. SIAM, 2005, pp. 606–610.
- [31] E. Luzhnica, B. Day, and P. Lio, "Clique pooling for graph classification," *International Conference of Learning Representations (ICLR) – Representation Learning on Graphs and Manifolds workshop*, 2019.
- [32] R. Ying, J. You, C. Morris, X. Ren, W. L. Hamilton, and J. Leskovec, "Hierarchical graph representation learning with differentiable pooling," *arXiv preprint arXiv:1806.08804*, 2018.
- [33] S. J. Hongyang Gao, "Graph u-nets," in *Proceedings of the 36th International conference on Machine learning (ICML)*, 2019.
- [34] C. Cangea, P. Velicković, N. Jovanović, T. Kipf, and P. Liò, "Towards sparse hierarchical graph classifiers," in *Advances in Neural Information Processing Systems – Relational Representation Learning Workshop*, 2018.
- [35] B. Knyazev, G. W. Taylor, and M. R. Amer, "Understanding attention in graph neural networks," *arXiv preprint arXiv:1905.02850*, 2019.
- [36] E. Noutahi, D. Beani, J. Horwood, and P. Tossou, "Towards interpretable sparse graph representation learning with laplacian pooling," *arXiv preprint arXiv:1905.11577*, 2019.
- [37] F. Diehl, T. Brunner, M. T. Le, and A. Knoll, "Towards graph pooling by edge contraction."
- [38] F. Diehl, "Edge contraction pooling for graph neural networks," *CoRR*, vol. abs/1905.10990, 2019. [Online]. Available: <http://arxiv.org/abs/1905.10990>
- [39] F. Gama, A. G. Marques, G. Leus, and A. Ribeiro, "Convolutional neural network architectures for signals supported on graphs," *IEEE Transactions on Signal Processing*, vol. 67, no. 4, pp. 1034–1049, 2018.
- [40] D. P. Kingma and J. Ba, "Adam: A method for stochastic optimization," *International Conference on Learning Representations (ICLR)*, 2015.
- [41] N. Shervashidze, P. Schweitzer, E. J. v. Leeuwen, K. Mehlhorn, and K. M. Borgwardt, "Weisfeiler-lehman graph kernels," *Journal of Machine Learning Research*, vol. 12, no. Sep, pp. 2539–2561, 2011.
- [42] T. Mikolov, I. Sutskever, K. Chen, G. S. Corrado, and J. Dean, "Distributed representations of words and phrases and their compositionality," in *Advances in Neural Information Processing Systems*, 2013, pp. 3111–3119.
- [43] N. Srivastava, G. Hinton, A. Krizhevsky, I. Sutskever, and R. Salakhutdinov, "Dropout: a simple way to prevent neural networks from overfitting," *The Journal of Machine Learning Research*, vol. 15, no. 1, pp. 1929–1958, 2014.
- [44] S. Hochreiter and J. Schmidhuber, "Long short-term memory," *Neural Computation*, vol. 9, no. 8, pp. 1735–1780, 1997.
- [45] A. v. d. Oord, S. Dieleman, H. Zen, K. Simonyan, O. Vinyals, A. Graves, N. Kalchbrenner, A. Senior, and K. Kavukcuoglu, "Wavenet: A generative model for raw audio," *arXiv preprint arXiv:1609.03499*, 2016.
- [46] S. Bai, J. Z. Kolter, and V. Koltun, "An empirical evaluation of generic convolutional and recurrent networks for sequence modeling," *arXiv preprint arXiv:1803.01271*, 2018.